

# REMOVAL OF EYE BLINK ARTIFACTS FROM THE EEG SIGNAL

Ivan Markovinović<sup>1\*</sup> - Saša Vlahinić<sup>1\*</sup> - Miroslav Vrankić<sup>1\*</sup>

<sup>1</sup>Department of Automatics and Electronics, Faculty of Engineering, University of Rijeka, Vukovarska 58, 51000 Rijeka

---

## ARTICLE INFO

### Article history:

Received: 11. 2. 2019.

Received in revised form: 15. 5. 2019.

Accepted: 16. 5. 2019.

Keywords:

EEG

Eye blink artifacts

Signal processing

ICA

ADJUST

DOI: <http://doi.org/10.30765/er.40.2.11>

---

### Abstract:

*Electroencephalography (EEG) is well known method of recording electrical brain activity with electrodes placed along the scalp. One of the challenging tasks in this field is the removal of electrical signals that are not related to brain activity.*

*In this paper, an algorithm for the removal of the EEG signals corresponding to the eye blink artifacts is presented. The presented algorithm is based on ADJUST artifact removing tool, which uses independent component analysis (ICA) for signal decomposition. For every signal component returned by the ICA algorithm, temporal-spatial features are calculated, upon which every independent component is classified as artifact or non-artifact, and removed accordingly.*

---

## 1 Introduction

Electroencephalography (EEG) is well known technique for acquiring electrical brain activity data [1]. Thanks to its temporal resolution and everyday declining cost of the EEG acquisition systems (in comparison to other brain activity acquisition systems like Magnetoencephalography (MEG)), the EEG is most widely distributed method of measuring human brain functionality.

Despite all of the virtues that EEG system poses, one of the main challenges in EEG acquisition processing is artifact removal. Physiological artifact activity like eye or neck movement, could potentially lead to extreme amplitude jumps that are 5-10 times greater than the normal brain activity measured by the EEG acquisition system. Such amplitude disturbances in the signal can obscure electrical brain activity of interest, leaving us with the challenging task of neurological and

physiological activity separation. Other type of artifacts are of a non-biological nature and are mainly caused by the electrode high-impedance or the electric device interferences.

Over the last decades numerous methods of non-neurological removal in the acquired EEG signal have been developed. One of the simplest methods is the threshold method, in which the samples with amplitudes greater than the threshold value are simply removed from the signal. Although this method is very simple and fast, the significant amount of information is lost in the remaining EEG signal. For the EEG signals that are decomposed into epochs, a simple averaging method over epochs can be used. However, this procedure is limited with the number of available averaging epochs and the artifact frequency.

Some advanced methods of the EEG artifact removal consist of modelling the eye blink or the ocular movement, and removing them from the

---

\* Corresponding author. Tel.: +385 51 505 720

E-mail address: [imarkovinovic@riteh.hr](mailto:imarkovinovic@riteh.hr)

original EEG signal. For this purpose, additional electrooculogram (EOG) channel is placed around eyes measuring the electrical activity of the eye muscles [2]–[4]. This signal combined with the propagation model of the artifact signal, can elicit a propagated artifact signal that can be easily subtracted from the artifact-corrupted EEG signal.

Most recent efforts in the field of artifact removal algorithms, involve independent component analysis (ICA) tool; a statistical tool which decomposes a multidimensional signal into the maximally independent components (IC) originating from independent signal sources [5], [6]. Because of its statistical approach and assumptions (eg. linear mixing of ICs) a perfect signal decomposition is not always possible. Nevertheless, the EEG signals can be successfully decomposed with the ICA into independent components (IC) related to the various artifacts, which can then be subtracted from the original EEG signal.

In this paper we propose an algorithm for the eye blink artifact removal based on the Automatic EEG artifact Detection based on Joint Use of Spatial and Temporal features (ADJUST) tool. Compared to the ADJUST, the proposed algorithm involves extra steps, including eye blink artifact detection and decomposition of the EEG signal into the signal epochs containing artifact and nearby clean brain activity samples. The extracted epochs are then decomposed with the ICA into ICs which have been classified into artifact and non-artifact classes, based on their spatial-temporal features. Guided with the ICA limitations stated before, the iterative ICA, the spatial-temporal features calculation and the IC classification process is implemented in the proposed algorithm, ensuring better artifact rejection.

## 2 The acquisition system of the EEG signals and experiment design

Datasets used for the development and analysis of the proposed artifacts removing algorithm, have been collected from the candidates participating in a typical auditory event-related potential paradigm. The experiment is designed in OpenVibe [7] and consists of six different words that are randomly played on the speaker. One of the events represents the target event, while the other events are labelled as non-targets. For the purpose of this paper, the candidates have not just focused on the played

words, but were also asked to make an eye blink whenever they hear the target event.

The EEG measurements have been collected with 2 different EEG data acquisition systems the Emotiv Epoc+ and the Brain Products V-Amp. The Emotiv Epoc+ [8] is an accessible and cheap EEG acquisition system, with 14 EEG signal electrodes, one reference, one ground electrode (Fig. 1), and maximal sampling frequency of 128 Hz. V-Amp [9] on the other hand is high-quality device for the EEG acquisition, with 16 EEG electrodes, one reference, one ground electrode, 24-bit AD converter, and 512 Hz sampling frequency. The main advantage of the V-Amp system over the Emotiv Epoc+ system, beside the technical specifications, is the ability of setting custom electrode configuration (Fig. 2).

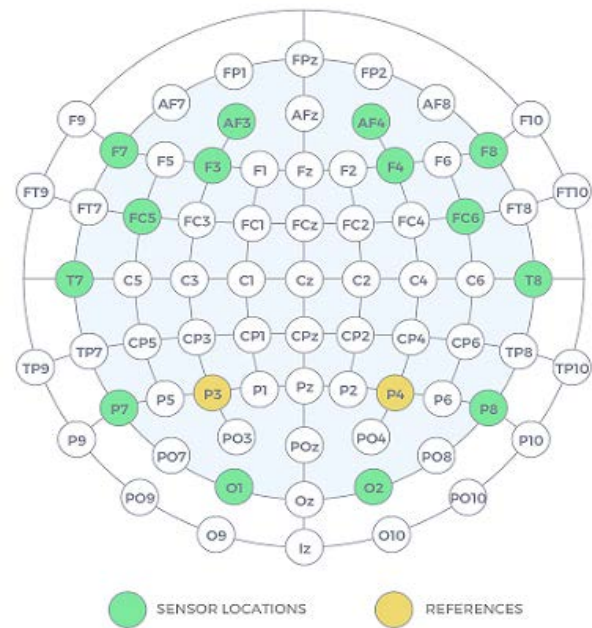


Figure 1. The position of the electrodes in the Emotiv Epoc+ EEG [8] acquisition systems. Used signal electrodes have been marked with green color

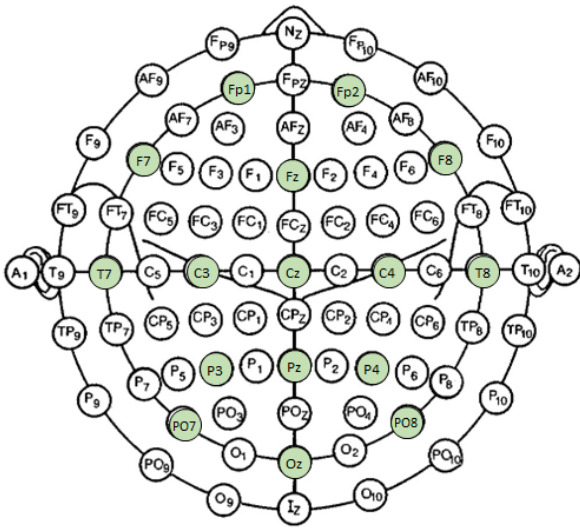


Figure 2. The position of the electrodes in the V-Amp 16 EEG acquisition systems. Used electrodes have been marked with green color

### 3 The ADJUST algorithm

The ADJUST [10] is a plugin tool for EEGLAB software [11] and is used for the removal of EEG artifacts from the EEG datasets. The main advantage of the ADJUST algorithm is the ability to automatically decompose a set of multidimensional EEG signals into ICs, classifying them as artifacts and non-artifacts and removing artifact related ICs without any user intervention or supervision. The ADJUST algorithm can distinguish 4 different EEG artifacts corresponding to the: eye blink (EB), vertical eye movement (VEM), horizontal eye movement (HEM) and generic discontinuities (GD), related to the problems with a EEG data acquisition system.

As stated in the introduction, only removal of the eye blink artifacts will be a subject of this research. Fig 3. shows a block diagram of the new enhanced algorithm for the removal of eye blink artifacts based on the ADJUST algorithm. Blocks marked with the green color are original ADJUST functions for the decomposition, temporal and spatial feature calculation and classification, which have been explained in continuation of this section.

#### 3.1 The independent component analysis

The ICA algorithm is a statistical method for decomposition of the observed multidimensional

random vector into components which are statistically as independent from each other as possible. For our particular problem, the ICA algorithm will decompose  $N$ -dimensional EEG signal into  $N$  ICs, which are product of the  $N$  independent brain activity sources [5], [6]. Beside the ICs, a mixing matrix  $A$  is returned satisfying the following equation:

$$EEG = A * IC \quad (1)$$

where  $EEG$  is measured  $N$ -dimensional EEG signal, and  $IC$  is  $N$ -dimensional vector of brain source independent components.

Applying the principal component analysis (PCA) on data before execution of the ICA algorithm, the number of desired ICs is reduced, simplifying the component extraction process.

#### 3.2 Spatial and temporal classification features

For discrimination between the eye blink artifacts and the non-artifact, ICs spatial and temporal features of independent components are calculated based on the ICA outputs.

##### 3.2.1 Spatial average difference

By their nature, the eye blink artifacts induce a high voltage jumps in frontal area of the brain. Thus in order to distinguish artifacts from non-artifact a measure is introduced, which emphasizes amplitude jumps of EEG signal in the frontal areas, and suppressing the jumps on electrodes covering the posteriori region of the brain. Accordingly, the spatial average difference (SAD) calculated for each IC is defined as following [10]:

$$SAD = |avg(A_{FA})| - |avg(A_{PA})| \quad (2)$$

where  $A_{FA}$  and  $A_{PA}$  represents the vectors of normalized ICA mixing matrix weights of frontal and posteriori electrodes, respectively and  $avg$  denotes the averaging function. This feature is calculated for every IC.

Similar to the SAD, one more control variable called Spatial Variance Difference (SVD) is introduced and defined as following [10]:

$$SVD = var(A_{FA}) - var(A_{PA}) \quad (3)$$

where *var* denotes a variance function. Because of the high amplitude oscillations and spatial distribution of the eye blinking artifacts, the variance of signals measured in frontal area should be larger than the variance of posteriori EEG signals, resulting in a positive SVD for the ICs originating from eye blink artifacts. This control variable is useful in situations where the mixing matrix weights across the posteriori electrodes have positive and negative values, leading to a very low average value of the posteriori mixing matrix weights. This could potentially lead to a false positive classification of ICs as the eye blinking artifact parts.

### 3.2.2 Temporal kurtosis

Kurtosis is widely used statistical method, based on the high-order statistics, which is very sensitive to outliers of the amplitude distribution, and is calculated as [10]:

$$Kurt[X] = E \left[ \left( \frac{X - \mu}{\sigma} \right)^4 \right] \quad (4)$$

where  $E$  stands for the expected value,  $X$  is a signal vector, and  $\mu$  and  $\sigma$  are mean value and standard deviation of vector  $X$ , respectively.

Combining the kurtosis with the property of high amplitude nature of the EEG artifact signal, it is reasonable assumption that the eye blinking artifacts are very well captured by this measure.

Thus, combining the kurtosis with the SAD feature will achieve better IC classification as artifacts and non-artifacts.

### 3.3 Features classification

The Expected-Maximisation algorithm [12] has been used in order to classify the ICs as artifacts and non-artifacts, based on the previously discussed temporal-spatial measures.

This algorithm takes the calculated features and separates them into two classes  $C^a$  and  $C^{na}$ , where  $C^a$  and  $C^{na}$  are the IC classes associated with artifacts and the brain activity sources, respectively. The separation is performed, by simply calculating the median value:

$$M = \frac{\max(C) + \min(C)}{2} \quad (5)$$

of whole feature space and classifying the feature values smaller than  $M$  into  $C^{na}$  class while the values larger than  $M$  into  $C^a$  class.

The created classes  $C^a$  and  $C^{na}$  have been used for calculation of two Gauss distributions, which intersection gives a threshold value for artifact and non-artifact feature separation. This procedure is then iterated until the difference between the calculated threshold values from the two consecutive steps is lower than the user pre-defined value. At every iteration of the Expected-Maximisation algorithm, the Gauss distribution statistics is updated by maximizing the log-likelihood measure.

By applying this method on the SAD measure and kurtosis we obtain two threshold values. The final classification of the ICs as artifacts is preformed if the component satisfies both threshold conditions.

## 4 Enhanced artifact removing algorithm

In order to get better removal of eye blink artifacts, some extra steps have been introduced around the ADJUST algorithm core and some existing ones have been modified (Fig. 3). The main reason behind the insufficient elimination of the artifacts can be interpreted by the ICA algorithm limitations and assumptions. For this reasons the extra steps in the proposed algorithm have been primarily focused on two goals:

- lowering the number of EEG samples that are subjected to the ICs analysis and signal processing methods;
- quality measure calculation of eye blink artifact removal algorithm for every detected eye-blink artifact.

### 4.1 The EEG data preprocessing

Before application of the artifact removing algorithm on the recorded datasets, datasets have been pre-processed. Firstly, datasets have been visually inspected and the corrupted parts of the signals have been removed. Secondly, DC component (mean value) of every channel has been computed and removed from the clean EEG signals. Thirdly, the EEG measurements have been filtered with the 16th order FIR bandpass filter with cut-off frequencies of 0.5 Hz and 40 Hz. In doing so, better linear signal decomposition results have been reported [13]. For this purpose, MATLAB *filtfilt*

function has been used, resulting in the filtered signal without the phase shift.

#### 4.2 Eye blink artifact detection method

Eye blinking artifacts are one of the worst disturbances in the EEG signals, which are

characterized by the abrupt amplitude jumps on the frontal electrodes of the EEG acquisition system, but can also lead to the amplitude jumps on all electrodes depending on the reference electrode position.

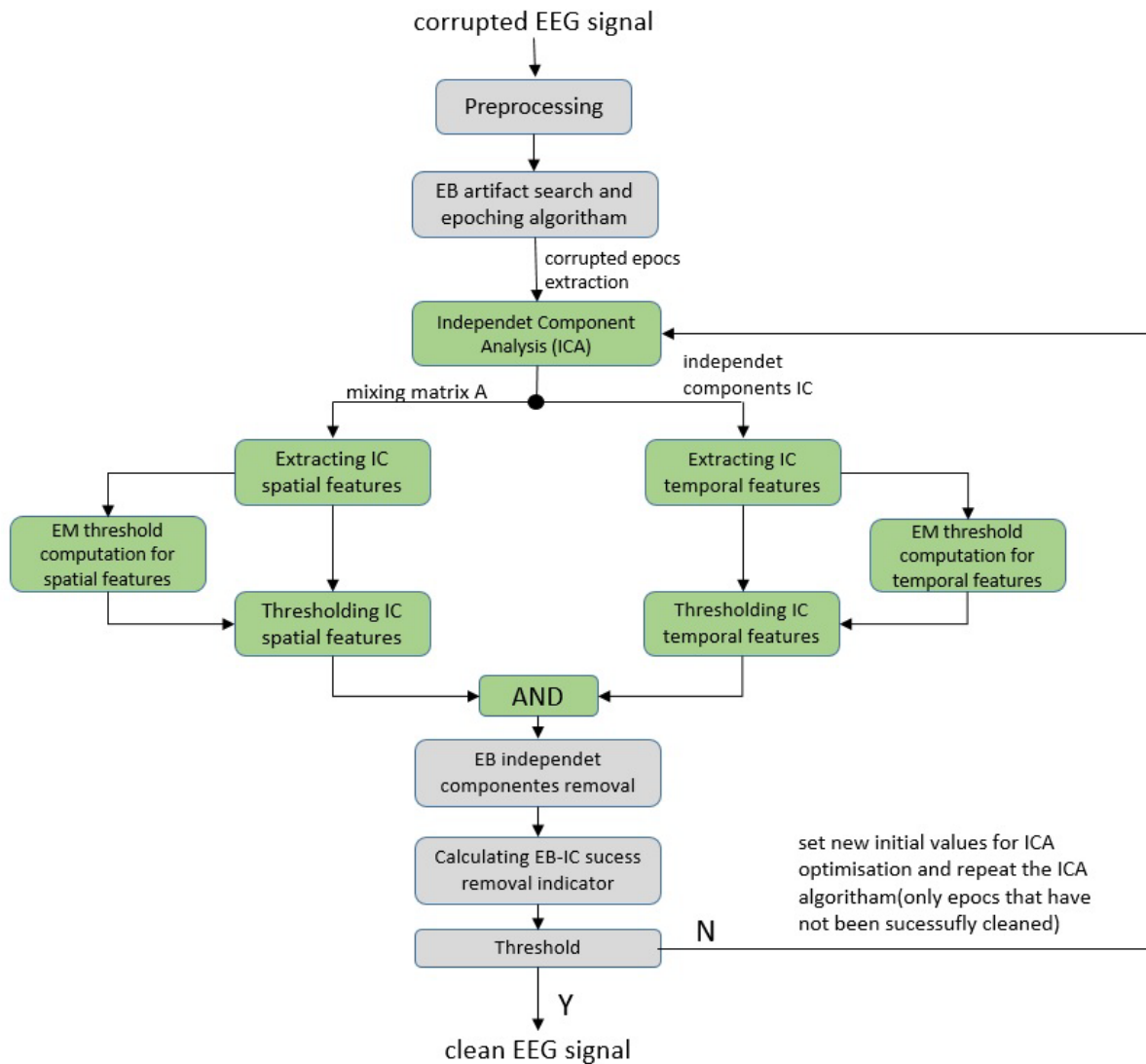


Figure 3. The block diagram of the proposed eye blink artifact removing algorithm

For rough detection of the blinking artifact locations, the simple peak detection method with threshold has been used. Depending on the acquisition system and the reference/ground electrode positions the peak detection has been applied on different electrodes. For the Emotiv EPOC+, four EEG signals from frontal electrodes (AF3, F3, AF4 and F4) have been summed up, enhancing the artifact to clean EEG signal ratio.

Because of the differences between the reference electrode positions in the V-Amp 16 and Emotiv EPOC+ acquisition systems as shown in Fig. 1 and Fig. 2, strong eye blink artifacts have been observed on all signal electrodes of the V-Amp system. With the same idea of enhancing artifact to clean EEG ratio in mind, signal from all electrodes of the V-Amp acquisition system have been summed up. By applying the peak detection algorithm on the summed signals, the positions of eye blink artifact peaks have been located. These sample values have been used, as a starting points for the signal epoching and the artifact removing process.

### 4.3 The EEG dataset epoching

The previously calculated sample markers have been used for extraction/epoching of the EEG signal parts affected by the eye blink artifacts. The idea behind epoching procedure is that the ICA algorithm is only executed over the epochs, containing the eye blink artifacts.

One of the most important conditions for the successful ICA is having enough data for IC extraction. Some empirical guidelines define the minimum number of samples for the successful and argumentative ICA as 20-30 times number of desired IC [14].

Following the mentioned guideline, we have developed a simple epoching algorithm, that is creating epochs of the same length around detected artifacts. The algorithm is trying to enclose one or more artifacts, depending on their sample distance. After the initial windows have been set, the algorithm will consecutively shift all epochs left and right until there is no more overlapping between the neighbouring epochs. Epochs shifting is a restrained action, which can potentially lead to ejection of the artifacts from the defined epoch. Following this restrain, epochs shifting is possible only under condition that all of the artifacts enclosed by the epoch initialization stay in the same epoch after a successful shift.

However, it is not always possible to surround the artifacts with the selected epoch length without overlapping between neighbouring epochs, therefore in those situations the epoch length is reduced by the adjustable number of samples and the process is repeated until the algorithm has managed to set the epochs without the overlapping. Example of the EEG signal with the correctly calculated epochs is shown in Fig. 4.

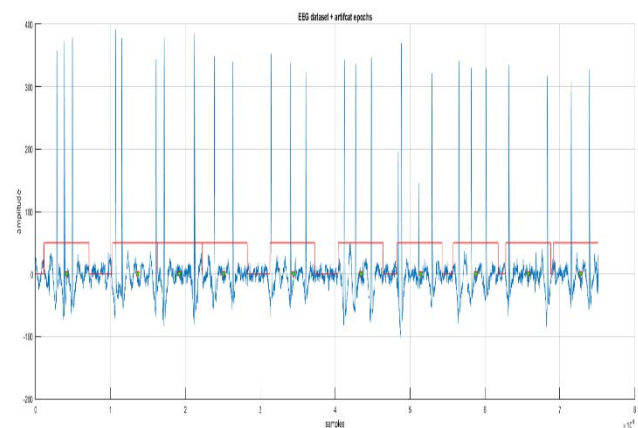


Figure 4. The EEG data for the Fp1 electrode (blue signal) and final artifact epoch positions (red signal) after the completion of artifact epoching algorithm. All artifacts are surrounded by their corresponding epoch without any overlapping

### 4.4 Independent component extraction and feature calculation

After the EEG pre-processing and epoching, the algorithm steps for the IC extraction, the spatial-temporal feature calculation, and classification of the extracted ICs are analog to the ADJUST algorithm.

Two steps of the ADJUST algorithm have been modified, and are discussed down below.

#### 4.4.1 Electrode selection for spatial and temporal features

Applying the channel selection guidelines introduced in the ADJUST algorithm [10], [15] on our EEG acquisition systems, the following electrodes/channels have been chosen to fill the frontal and posteriori channel vectors, respectively. For the Emotiv EPOC+ acquisition system we have selected the following frontal area (FA) and posteriori area (PA) electrodes:

FA = [AF3(Ch1), F3(Ch3), F4(Ch12), AF4(Ch14)],  
 PA = [P7(Ch6), O1(Ch7), O2(Ch8), P8(Ch9)],

while for the V-Amp 16 acquisition system, the following electrodes have been selected:

FA = [Fp1(Ch1), Fp2(Ch2), F3(Ch3), Fz(Ch4),  
 F4(Ch5)],  
 PA = [P3(Ch11), Pz(Ch12), P4(Ch13), PO7(Ch14),  
 Oz(Ch15), PO8(Ch16)].

For the selected electrode vectors, the spatial and temporal features and related threshold values have been calculated as explained in Section 3.

#### 4.4.2 The independent components analysis

For our purposes the Fast ICA (FICA) algorithm [6], [16] has been used. The FICA algorithm is applied on all epochs with the PCA dimension reduction (typ. 12 ICs have been extracted per epoch). Default outputs of the FICA function are the mixing matrix  $A$ , the weight matrix  $W$  (inverse of the mixing matrix  $A$ ) and the independent components  $IC$ . Mentioned values have been used for spatial and temporal feature calculation associated with the eye blink artifacts.

In addition to those 3 default outputs, the 4<sup>th</sup> output has been added and defined as a convergence success indicator. This indicator indicates that the FICA convergence has not been successful and that the given FICA results are not correct. The FICA algorithm will be repeated until the successful convergence or the maximum allowed number of iterations. In every new iteration, a new initial value of the mixing matrix  $A$  for FICA algorithm will be generated. If the maximal number of FICA attempts has been reached, without successful IC extraction, the affected epochs are marked and skipped by the artifact removing algorithm.

#### 4.5 Artifact removal and success indicator calculation

With the calculated feature threshold values, all of the ICs can be classified as artifacts if both features are larger than the respective threshold value, and as non-artifact otherwise.

The ICs which are classified as artifact are then removed from the EEG signal. In order to avoid sharp edges in processed signal, caused by the removal of the artifact related ICs, low-pass filter has been applied to the EEG signal.

After removal of the artifact related ICs from the EEG signal, for every epoch and every artifact, the artifact removal success indicator has been calculated. This indicator is used for the detection of the artifact areas that have not been properly processed, and further iterations are necessary to ensure a valid result. As mentioned before, the artifact epochs contain one or more artifacts, which are surrounded by their respective markers. All other samples in that epoch can be interpreted as the “clean” EEG signal, as shown in Fig 5. First step of the indicator calculation is to take clean parts of the EEG signal in the associated epoch and calculate the mean value and variance.

The calculated variance of the signal represents the energy distribution of the “clean” EEG signal parts. The calculated mean value is then used for the variance calculation on the samples which are bounded within artifact markers. The calculated variance can be interpreted as the energy distribution of the corrected signal. It is a reasonable assumption that energy of the EEG signal containing artifacts (or artifact remains), is significantly higher than the “clean” EEG. This assumption combined with simple threshold logic, has been used as a measure for the inadequate artifact removal.

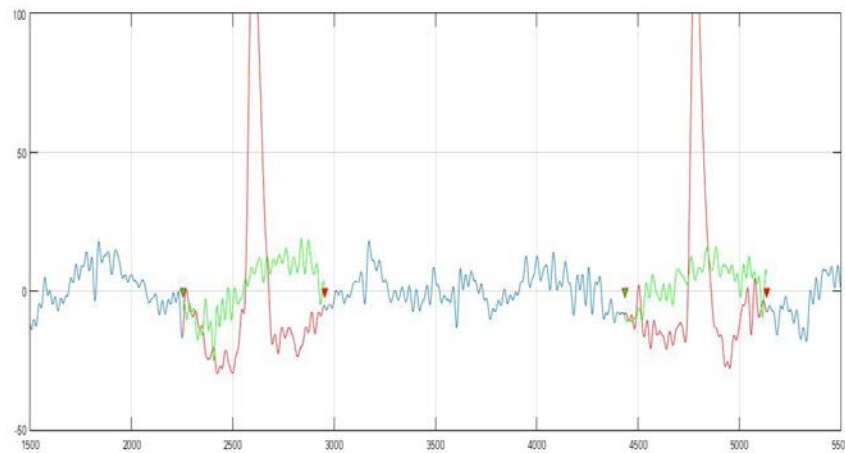


Figure 5. Illustration of the artifact epoch containing two artifacts. The green and red triangles represent the left and right artifact markers, respectively. The blue colored signal is associated with the “clean” EEG signal, where red colored signal is associated with the eye-blink artifacts. If the artifact removal algorithm has been successful, energy distributions of green signals should be similar to the signal distribution of the blue signal

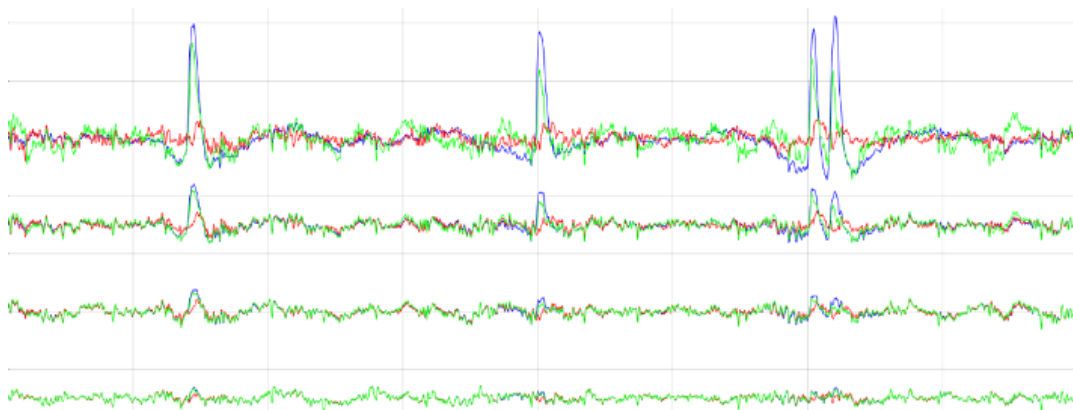


Figure 6. Fraction of the EEG signal after the artifact removal with the ADJUST (green line) and the proposed artifact removal algorithm (red line) on the Fp1, Fz, Cz and Pz electrodes. The blue line represents the original EEG signal corrupted with the eye blink artifacts

#### 4.6 Improving removal results

If the “artifact” energy is significantly larger than the energy of the “clean” EEG signal, the associated epochs will be marked as “unsuccessfully cleaned” and the artifact removal algorithm will be repeated on that epoch. This includes a new execution of the FICA algorithm, calculation of new classification features, and the calculation of success indicator.

The main reason behind the unsuccessful artifacts removal is most likely the ICA, caused by its statistical approach, simplifications and assumptions (eg. equal or less number of electrodes and active

sources, linearity, etc.). In fact 50-70% of the returned ICs do not have a neurological interpretation [17].

For this reason, the unsuccessfully processed epochs are iteratively subjected to the removing algorithm until the necessary success indicator values are satisfied, or the maximum number of iterations has been reached.

## 5 The results

Validation of the proposed artifact removal algorithm has been conducted on 24 recordings,

recorded as explained in the Section 2. A ratio between the signal energies of clean EEG signal parts and the corrupted signal parts has been calculated in order to validate results for all trials on all electrodes. Furthermore, to get better view on performance of the proposed algorithm, the energy ratios have been compared with the energy ratios of the EEG recordings processed by the open-source EEGLAB plug-in artifact removal algorithms: Automatic Artifact Removal tool (AAR) [18], ADJUST, Multiple Artifact Rejection Algorithm (MARA) [19][20], Fully Automated Statistical Thresholding for EEG artifact Rejection (FASTER) [21]. Due to fact that the FASTER tool is a high density EEG artifact removal algorithm for the acquisition systems with more than 32 electrodes, no comparison between the algorithms has been conducted.

Applying the MARA artifact removal algorithm on the EEG recordings, by removing all artifacts from the EEG signal, but at cost of removing almost all essential neurological parts. This is very pronounced

on the frontal electrodes, as it can be seen from Fig. 7. The reason for such performance is that the MARA classifier marked 15 out of possible 16 ICs, returned by the ICA algorithm, as artifacts. As reported in [19] the MARA algorithm has been validated on different EEG recordings with electrode sets that covered the entire scalp with the approximately equidistant electrode positioning. However, the performance of the MARA algorithm has not been analysed on the EEG acquisition systems with the reduced number of electrodes. From the presented results we can only conclude that the MARA algorithm performed extremely aggressive on the low-density EEG recordings, and thus, the MARA algorithm is not suitable for the EEG electrode configurations used in this paper. Improvement of the results can be achieved by the manual inspection and classification of the artifact related ICs. However, the proposed algorithm is fully automated, and thus, no further comparison between the MARA algorithm and proposed artifact removing algorithm has been conducted.

Table 1. The artifact removal results with the proposed artifact removing algorithm (ARA), the ADJUST (ADJ) algorithm, and the AAR algorithm for 6 different recordings. For each recording and channel, energies of the clean EEG signal parts and the corrupted EEG signal parts have been calculated after the artifact removal, and shown in energy ratio form. Last column represents the grand-mean over all recordings

Trial nCh	1			2			3			4			5			6			mean		
	ARA	ADJ	AAR	ARA	ADJ	AAR	ARA	ADJ	AAR	ARA	ADJ	AAR	ARA	ADJ	AAR	ARA	ADJ	AAR	ARA	ADJ	AAR
Fp1	1,61	1,28	1,38	1,40	0,16	0,20	1,47	5,65	8,55	0,79	0,79	0,08	2,09	1,02	0,70	1,34	1,19	0,54	1,45	1,68	1,91
Fp2	1,55	1,12	1,14	1,06	0,14	0,11	1,56	4,18	4,06	0,57	0,70	0,06	1,72	1,04	0,48	1,10	1,20	0,50	1,26	1,40	1,06
F3	0,83	0,71	1,71	0,97	0,14	0,14	0,83	1,85	1,80	0,58	0,32	0,08	0,79	0,64	0,48	0,47	0,49	0,15	0,75	0,69	0,73
Fz	0,92	0,65	1,77	0,73	0,11	0,11	0,86	3,96	1,81	0,33	0,25	0,06	0,62	0,49	0,46	0,47	0,20	0,11	0,65	0,95	0,72
F4	0,83	0,83	1,64	0,75	0,12	0,12	0,71	3,43	1,59	0,21	0,31	0,10	0,57	0,50	0,32	0,42	0,76	0,49	0,58	0,99	0,71
T7	1,29	1,26	2,44	2,02	0,32	0,22	1,30	9,92	20,37	1,14	0,09	0,11	0,36	0,37	0,55	0,24	0,15	0,42	1,06	2,02	4,02
C3	0,77	0,51	2,46	0,21	0,15	0,12	0,68	0,66	5,58	0,36	0,16	0,15	0,39	0,43	1,15	0,26	0,26	0,30	0,45	0,36	1,63
Cz	0,72	0,48	1,72	0,85	0,10	0,13	0,71	3,56	0,77	0,24	0,10	0,08	0,44	0,51	0,54	0,31	0,22	0,36	0,54	0,83	0,60
C4	0,61	0,48	1,50	0,48	0,08	0,09	0,54	4,08	0,99	0,16	0,09	0,08	0,32	0,56	0,37	0,20	0,16	0,23	0,38	0,91	0,54
T8	0,47	0,32	1,20	0,10	0,04	0,04	0,38	0,61	4,38	0,33	0,06	0,03	0,15	0,24	0,15	0,12	0,15	0,19	0,26	0,24	1,00
P3	2,45	4,14	4,92	0,45	0,14	0,11	0,62	1,37	7,55	0,25	0,08	0,12	0,36	0,37	0,50	0,30	0,23	0,31	0,74	1,05	2,25
Pz	0,68	0,38	1,67	0,96	0,09	0,23	0,64	1,62	0,79	0,22	0,07	0,08	0,37	0,78	0,37	0,25	0,27	0,33	0,52	0,53	0,58
P4	0,50	0,49	1,48	0,42	0,15	0,09	0,46	4,17	0,40	0,15	0,04	0,05	0,25	0,43	0,41	0,22	0,24	0,40	0,33	0,92	0,47
PO7	0,72	0,63	1,69	0,47	0,11	0,12	0,82	1,23	4,00	0,88	0,07	0,08	0,34	0,49	0,79	0,22	0,13	0,14	0,58	0,44	1,14
Oz	0,69	0,29	2,59	1,34	0,27	0,15	1,69	2,69	50,03	0,44	0,06	0,07	0,36	0,29	0,56	0,22	0,17	0,25	0,79	0,63	8,94
PO8	0,43	0,22	1,36	0,20	0,04	0,05	0,24	0,63	1,05	0,15	0,03	0,04	0,11	0,16	0,24	0,11	0,06	0,13	0,21	0,19	0,48

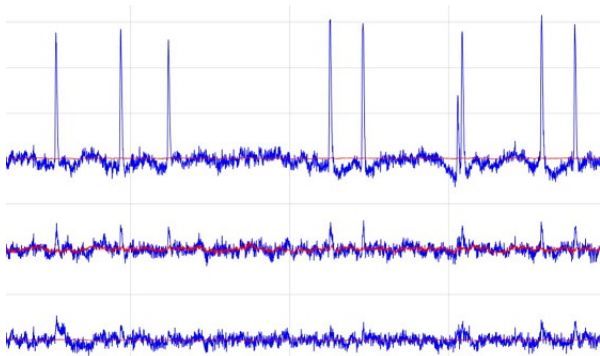


Figure 7. Fraction of the EEG signal after the artifact removal with the MARA tool (red line) on Fp1, Cz and Pz electrodes, respectively. Blue lines represent the original corrupted EEG signals

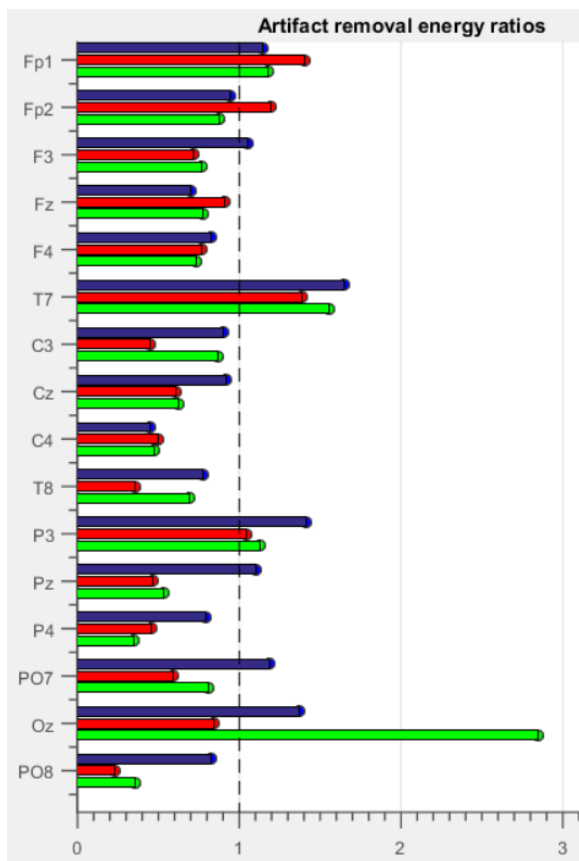


Figure 8. The energy ratio for all electrodes on all 24 recordings after the EEG data has been processed with the following artifact removing algorithms: ARA (blue bars), ADJUST (red bars), AAR (green bars). The dotted line represents ideal energy ratio after the artifact removal process

Compared to the ADJUST artifact removing algorithm, the ability of proposed algorithm to repeat the artifact removal process on “unsuccessfully cleaned” epochs, provided better artifact removal results, as shown in Fig. 6. Table 1. shows the energy ratios between the clean and the corrupted EEG signal areas over all EEG channels for the proposed removal algorithm (ARA), and the EEGLAB plug-in artifact removal tools: ADJUST and AAR. For the ratio value equal to one, a reasonable assumption is that the artifact removal process has been ideal due to the fact that energies of the compared signal parts are equal. On the other hand, if ratio values are higher than one, the corrupted signal areas are over-filtered, or under-filtered if the ratio values are lower than one.

Figure 8. shows the energy ratio comparison between the proposed artifact removal algorithm and the EEGLAB plug-in artifact removal tools: ADJUST and AAR, respectively. As shown, the proposed algorithm has achieved better results on almost all electrodes of used acquisition system. For the T7, P3, PO7, Oz electrodes, the energy ratios differ considerably from the ideal energy ratio value. This can be interpreted as the inability of the ICA algorithm to decompose signals on the highlighted electrodes into the ICs which can be classified as artifacts. In order to fully understand how the epoch length, different ICA algorithms and different classification methods can be optimised for achieving better artifact removing results, signals from those electrodes will be a focus point of our future research.

## 6 Conclusion

In this paper we have proposed the artifact removal algorithm based on the ADJUST algorithm. In order to get better artifact removal results we have modified the original algorithm by adding extra processing steps. The proposed algorithm can achieve better results through energy difference inspection between the “clean” and the processed signal parts and additional iterations of the artifact removal process on the artifact corrupted epochs, which have not satisfied the energy difference condition. In the experimental section we have shown that the proposed algorithm has achieved better results compared to the ADJUST algorithm on almost all electrodes.

Moreover, the ability of the proposed artifact removal algorithm to place epochs around the artifact peaks and process only samples inside the corrupted epochs is one more advantage of this approach. By doing so,

all samples outside the corrupted epochs have not been processed, leaving the original artifact-free EEG signal intact. Although many advanced artifact removing algorithms like MARA and FASTER have been introduced over the last years, they were unable to properly clean the EEG signal from the eye blink artifacts, for the electrode configurations used in this paper. Therefore, additional investigation of the artifact removal algorithms in the low-density EEG acquisition systems is necessary.

## References

- [1] Sanei, S., Chambers, J. A.: *EEG Signal Processing*, John Wiley & Sons, Ltd., Chichester, UK, 2007.
- [2] Croft, R. J., Barry, R. J.: *Removal of ocular artifact from the EEG: a review*, *Neurophysiology Clin.*, 30 (2000), 5–19.
- [3] Wallstrom, G. L., Kass, R. E., Miller, A., Cohn, J. F., Fox, N. A.: *Automatic correction of ocular artifacts in the EEG: a comparison of regression-based and component-based methods*, *Int. J. Psychophysiol.*, 53 (2004), 105–119.
- [4] He, P., Wilson, G., Russell, C.: *Removal of ocular artifacts from electroencephalography by adaptive filtering*, *Med. Biol. Eng. Comput.*, 42 (2004), 407–412.
- [5] Comon, P., Jutten, C.: *Handbook of Blind Source Separation*, Independent Component Analysis and Applications, Academic Press, Oxford, UK, 2009.
- [6] Hyvaerinen, A., Erkki, O.: *Independent Component Analysis: Algorithms and Applications*, *Neural Networks*, 13 (2000), 411–430.
- [7] OpenVibe, Software for Brain Computer Interfaces and Real Time Neuroscience 2015. <http://openvibe.inria.fr>. [10-May-2018].
- [8] Emotiv, EMOTIV EPOC+ 14 Channel Mobile EEG - Emotiv, <https://www.emotiv.com/product/emotiv-epoc-14-channel-mobile-eeeg/#tab-description>. [25-Apr-2019].
- [9] BrainProducts, “V-Amp.” [Online]. <https://www.brainproducts.com/productdetails.php?id=15>. [20-Apr-2019].
- [10] Mognon, A., Jovicich, J., Bruzzone, L.: *ADJUST: An automatic EEG artifact detector based on the joint use of spatial and temporal features*, *Psychophysiology*, 48 (2011), 229–240.
- [11] Delorme, A., Makeig, S.: *EEGLAB: An open source toolbox for analysis of single-trial EEG dynamics including independent component analysis*, *J. Neurosci. Methods*, 134 (2004), 9–12.
- [12] Bruzzone, L., Prieto, D. F.: *Automatic analysis of the difference image for unsupervised changed detection*, *IEEE Trans. Geosci. Remote Sens.*, 38 (2000), 1171–1182.
- [13] Frølich, L., Dowding, I.: *Removal of muscular artifacts in EEG signals: a comparison of linear decomposition methods*, *Brain Informatics*, 5 (2018), 13–22.
- [14] EEGlab, *Enough data points for ICA*, 2015. <https://sccn.ucsd.edu/pipermail/eeglablist/2015/009724.html>. [20-Sep-2017].
- [15] Mognon, A., Buiatti, M.: *ADJUST Tutorial An Automatic EEG artifact Detector based on the Joint Use of Spatial and Temporal features: A Tutorial*, [https://www.nitrc.org/docman/view.php/739/2101/TutorialADJUST1\\_1.pdf](https://www.nitrc.org/docman/view.php/739/2101/TutorialADJUST1_1.pdf)
- [16] Hyvaerinen, A., Erkki, O.: *A Fast Fixed-Point Algorithm for Independent Component Analysis*, *Neural Comput.*, 9 (1997), 1483–1492.
- [17] Delorme, A., Palmer, J., Onton, J., Oostenveld, R., Makeig, S.: *Independent EEG Sources Are Dipolar*, *PLoS One*, 7, 2012.
- [18] Gomez-Herrero, G., Anwar, H., Egiazarian, K.: *Automatic Removal of Ocular Artifacts in the EEG without an EOG Reference Automatic Removal of Ocular Artifacts in the EEG without an EOG Reference Channel*, *Signal Processing Symposium, 2006. NORSIG 2006. Proceedings of the 7th Nordic, 2006*.
- [19] Winkler, I., Haufe, S., Tangermann, M.: *Automatic Classification of Artifactual ICA-Components for Artifact Removal in EEG Signals*, *Behav. Brain Funct.*, 7 (2011), 30, 1–15.
- [20] Winkler, I.: *MARA Tutorial*, <https://irene.github.io/artifacts/>
- [21] Nolan, H., Whelan, R., Reilly, R. B.: *FASTER: Fully Automated Statistical Thresholding for EEG artifact Rejection*, *J. Neurosci. Methods*, vol. 192 (2010), 1, 152–162.